

Synthesis of Iron doped Manganese Cobaltite Nanoparticles for Supercapacitor Application

DIKSHA, DIKSHA KUMARI, RITESH KUMAR AND RAJESH KUMAR SINGH[†]

Department of Physics and Astronomical Science, Central University of Himachal Pradesh, Dharamshala (H.P.) 176215, India

Abstract. We have synthesized manganese cobaltite nanoparticles doped with iron (0.2, 0.4, 0.6) using a hydrothermal method. Crystal structure and the morphology of synthesized materials were characterized through X-ray diffraction (XRD) and field-emission scanning electron microscopy (FE-SEM). The presence of functional groups were examined using Fourier- transform infrared spectroscopy (FTIR). Additionally, electrodes of the samples were fabricated by using hydrothermal method to investigate their electrochemical properties. Electrochemical properties of prepared samples were evaluated with an electrochemical workstation employing two-electrode configuration in 3 M KOH electrolyte.

Keywords: Hydrothermal, Electrochemical properties, Supercapacitor

[†]Email: rsinghbhu@gmail.com

1. INTRODUCTION

In recent technological era, every aspect of our daily life is energy dependent. Our society faces energy and environmental challenges including pollution from toxic materials, limited availability of fossil fuels and the phenomenon of global warming. We need sustainable and clean energy sources and their associated technologies urgently to address these challenges [1]. Since these renewable energy sources are generally dependent on natural sources hence the energy from these sources has to be stored. Since supercapacitors and lithium-ion batteries have developed significantly in recent years, allowing for greater advancements in energy storage, there is a great deal of interest in increasing these technologies.

Supercapacitors have garnered a lot of attention because of their significant charge storage capacity, deliver high power, safety, absence of memory effect [2]. Supercapacitors are divided into two main types based on how they store charge: Electric Double Layer Capacitors (EDLCs) and Pseudocapacitors. In EDLCs, charge is stored by gathering on the surface of the electrodes. In pseudocapacitors, charge is stored through faradic redox reactions that occur at interface between the electrode and the electrolyte. Pseudocapacitors generally exhibit higher specific capacitance due to their dependence on faradaic processes [3,4].

Binary metal oxides are considered highly viable materials for pseudocapacitor electrodes. This interest is because of their excellent electrical performance and low cost [5]. For usage in Li-ion batteries and supercapacitors for energy storage, the MnCo_2O_4 spinel structure has drawn a lot of interest because of its superior specific capacity, natural availability, affordability and environmental friendliness [6] and its performance can be further enhanced by doping it with other transition metals. Several MnCo_2O_4 shapes have been produced and investigated for applicability as supercapacitor electrodes, according to the literature review. Sahoo et al. produced MnCo_2O_4 nanoparticles with capacitance values of 290 Fg^{-1} on indium tin oxide and 95.6 Fg^{-1} on nickel foam [7]. Li et al. achieved 349.8 Fg^{-1} with MnCo_2O_4 nanowires on nickel foam [8], while Thorat et al. reported 950 Fg^{-1} with MnCo_2O_4 microspheres at 2 Ag^{-1} [9].

This work focuses on the synthesis of iron (Fe) doped manganese cobaltite (MnCo_2O_4) nanoparticles using the hydrothermal method. The morphological and structural properties are being studied by Field emission scanning electron microscopy, Fourier transform infrared spectroscopy and X-Ray diffraction. Electrochemical performances are studied by cyclic voltammetry technique.

2. EXPERIMENTAL DETAILS

2.1 Materials used

We employed analytical-grade chemicals in our synthesis; no additional purification was performed. Manganese chloride tetrahydrate

($\text{MnCl}_2 \cdot 4\text{H}_2\text{O}$), Iron nitrate nonahydrate ($\text{Fe}(\text{NO}_3)_3 \cdot 9\text{H}_2\text{O}$), Cobalt nitrate hexahydrate ($\text{Co}(\text{NO}_3)_2 \cdot 6\text{H}_2\text{O}$), ammonia, NMP (N-Methyl-2-pyrrolidone), acetylene black and potassium hydroxide (KOH). Merck India provided all of the chemicals. Double distilled water was used throughout the synthesis and characterization process.

2.2 Synthesis of iron doped manganese cobaltite nanoparticles

The general formula for the nanoparticles, $\text{MnCo}_{2-x}\text{Fe}_x\text{O}_4$, was used during their production. The values of x can be 0.2, 0.4, or 0.6, which correspond to MCF 2, MCF 4, and MCF 6, respectively. First, a 1 M solution of nickel chloride was made in 25 milliliters of distilled water (referred to as solution A) in order to create MCF 2. In a similar manner, solutions B and C of 0.2 M and 1.8 M, respectively, of cobalt nitrate and iron nitrate, were made. After that, the solutions were combined and shaken for 30 minutes at room temperature with a magnetic stirrer. Then, NH_3 solution was added little by little to original mixture until solution's pH 12 was achieved. Subsequently, mixture was placed in a 100 ml autoclave and heated for 22 hours at 180°C . After this mixture cooled in autoclave, it was centrifuged multiple times using ethanol and DI water. Then, the precipitate was dried for 14 hours at 70°C in an oven. After that, the obtained material was calcined for five hours at 600°C in powder form. The process outlined for MCF 2 was also used to prepare the other samples, MCF 4 and MCF 6.

2.3 Characterization techniques

Crystallinity was assessed using X-ray diffraction (XRD) with a Panalytical Xpert Pro diffractometer, utilizing a $\text{CuK}\alpha$ X-ray source. To analyze the nanoparticles' morphology, field-emission scanning electron microscope (FESEM JSM 7900F, JEOL) was employed. The Fourier-transform infrared (FTIR) spectroscopy was performed using a Perkin Elmer spectrometer.

2.4 Electrode fabrication

Electrochemical performance of the synthesized electrode materials were studied by using a standard two-electrode setup. This investigation was conducted with an electrochemical workstation (CHI 760). To make the

electrodes, a mixture was created using $\text{MnCo}_{2-x}\text{Fe}_x\text{O}_4$, Acetylene Black, and Polyvinylidene Fluoride in an 80:10:10 ratio. This mixture was then dissolved in N-methyl-pyrrolidone. After that, the uniform slurry was coated onto the nickel foam, and it was vacuum-dried at 60°C for 12h. The prepared symmetric electrodes were put together into a cell setup using 3M KOH electrolyte. The Whatman filter paper served as a partition between the electrode to prevent them from touching each other. The constructed cell was placed within a Swagelok cell holder, and measurements of its electrochemical performance were made.

3. Results and Discussion

3.1 X-ray diffraction analysis

The Fig.1 displays diffraction peaks at 2Θ values of 18.39° , 30.33° , 35.97° , 43.50° , 53.68° , 57.26° and 62.95° corresponding to the crystal planes (111), (220), (311), (400), (422), (511), and (440) respectively. Furthermore, presence of an additional peak can be seen at 21.6° in the XRD patterns of MCF 2 and MCF 4, which is caused by the dopants forming a secondary phase. The sample's XRD pattern can be indexed using the JCPDS card number 23-1237 [10], which corresponds to MnCo_2O_4 with cubic structured spinel compound.

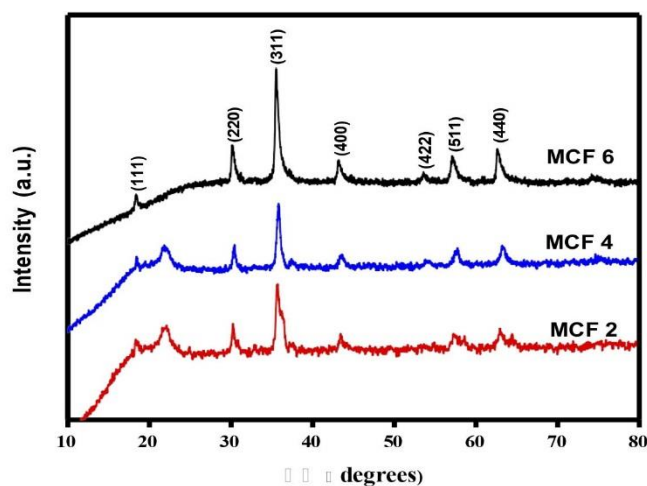


Fig 1: XRD pattern of MCF 2, MCF 4, MCF 6 nanoparticles.

The crystallite size of the MCF 2, MCF 4 and MCF 6 were determined using the Scherrer equation [11]:

$$D = \frac{k\lambda}{\beta \cos\theta} \quad (1)$$

Where D is the average crystallite size, k (0.9) is form factor, λ is the wavelength (0.154 nm) of the incoming X-rays of Cu K_{α} radiation, β is the full width half maximum of diffraction peak and θ is the Bragg diffraction angle. Crystallite sizes determined for MCF 2, MCF 4 and MCF 6 are approximately 15.45 nm, 26.51 nm, and 24.54 nm, respectively. With increase in doping level crystallite size increase up to $x = 0.4$ (MCF 4) and then decrease at $x = 0.6$ (MCF 6). This maybe due to at lower doping concentrations, the substitution of dopant ions into the crystal lattice causes slight distortions, which can lower the energy barrier for grain growth. This helps the crystal size to grow. However, at higher doping concentrations, excessive dopant ions introduce significant lattice strain or defects. These defects disrupt the crystal structure and hinder growth, resulting in a smaller crystallite size.

3.2 Fourier Transform Infrared Spectroscopy Analysis

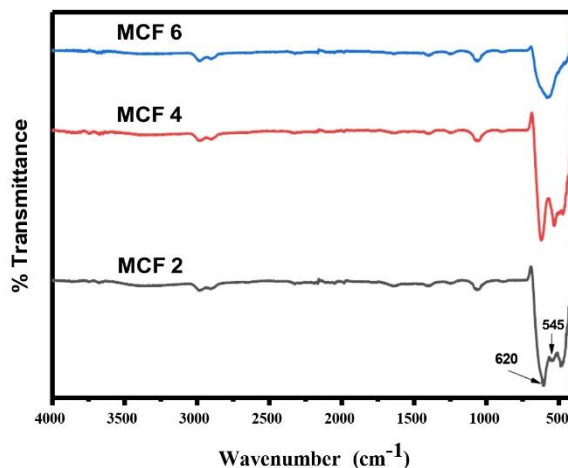


Fig 2: FTIR spectrum of MCF 2, MCF 4, MCF 6 nanoparticles

FTIR spectroscopy is a highly sensitive technique used to detect and identify various organic and inorganic functional groups in a sample. Using a wavelength range of 4000–400 cm^{-1} , the FTIR (using Perkin Elmer spectrometer) spectra of the MCF 2, MCF 4, and MCF 6 nanoparticles are displayed in Fig. 2. Two peaks in the fingerprint region indicate the presence of a Co–O bond at 545 cm^{-1} and a Mn–O bond at 620 cm^{-1} [12].

3.3 Field Emission Scanning Electron Microscope Analysis

Morphology of the sample surfaces was analyzed using a field emission scanning electron microscope (FESEM JSM 7900F, JEOL). The FESEM images of Fe doped MnCo_2O_4 nanoparticles, as displayed in Fig. 3 (a), (b), and (c) reveals that sample has an agglomerated nature and consists of nano crystals that appear as grain-like particles.

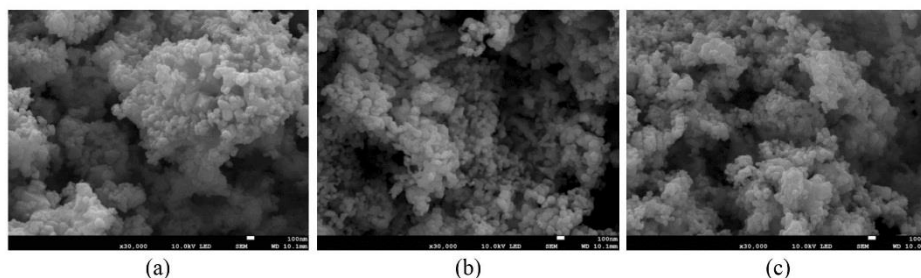


Fig 3: FESEM pictures of (a) MCF 2 (b) MCF 4 (c) MCF 6

The grain size for MCF 2, MCF 4 and MCF 6 were measured to be 61.56 nm, 56.91 nm and 58.83 nm, respectively.

3.4 Electrochemical Analysis

The three MCFs were developed as supercapacitor electrodes to evaluate their electrochemical performance. The electrodes' electrochemical behavior was investigated by using cyclic voltammetry (CV). Within potential ranges of -1 V to 1 V, cyclic voltammetry studies were conducted at various scan rates ranging from 5 mVs^{-1} to 60 mVs^{-1} . Fig. 4 displays the CV profiles of MCF 2, MCF 4 and MCF 6, which were acquired at various scan rates. Pseudocapacitive behavior of electrodes is indicated by redox peaks on the CV curves of each electrode in the KOH electrolyte solution (Fig. 4(a–c)).

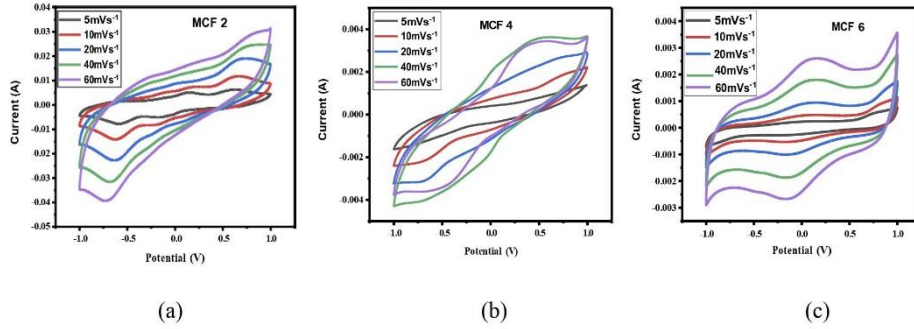


Fig 4: Cyclic voltammetry results for (a) MCF 2 (b) MCF 4 (c) MCF 6

As scan rate increases, positions of the peaks shift significantly, but the forms of the CV curves remain constant throughout a range of scan rates ($5\text{--}60\text{ mVs}^{-1}$). As a result, it has been observed that ionic and electronic movements occur more quickly at higher scan rates, which speeds up a redox reaction at interface between electrolyte and the electroactive material [13, 14].

Equation (2) can be used to compute specific capacitance (C_s) of built electrodes based on the CV graphs.

$$C_s = \frac{\int_{-v}^v I(v) dv}{S_r \times \Delta v \times m} \quad (2)$$

Here, m is mass of active material (g), S_r is scan rate (mVs^{-1}), I is the current (A), and Δv is voltage window. C_s is specific capacitance (Fg^{-1}).

The measured specific capacitance values at a 5 mVs^{-1} scan rate are 124.28 Fg^{-1} for MCF 2, 91.03 Fg^{-1} for MCF 4, and 54.58 Fg^{-1} for MCF 6. Table 1 presents specific capacitance values of MCF 2, MCF 4, and MCF 6 as obtained from the CV graph at the different scan rates.

Table 1. Specific capacitance values for MCF 2, MCF 4 and MCF 6 at different scan rates.

Scan Rates (mVs ⁻¹)	Specific Capacitance (Fg ⁻¹)		
	MCF 2	MCF 4	MCF 6
5	124.28	91.03	54.58
10	106.00	81.50	48.56
20	80.26	66.54	43.88
40	53.59	48.26	40.03
60	43.29	26.82	38.06

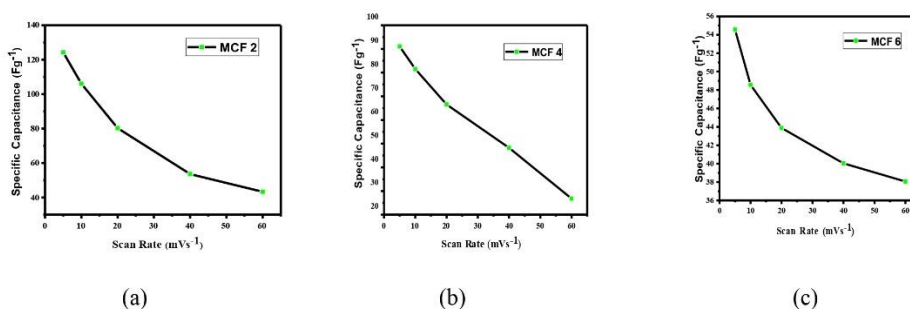


Fig 5: Specific capacitance Vs scan rate results for (a) MCF 2 (b) MCF 4 (c) MCF 6

The specific capacitance for MCF 2, MCF 4 and MCF 6 is found to decrease as the scan rates increase. This is because, at greater scan rates, the electrolyte ions travel more quickly, preventing them from completely engaging in the electrochemical interaction with the active material.

4. CONCLUSION

In summary, iron (0.2, 0.4, 0.6) doped MnCo_2O_4 nanoparticles (MCF 2, MCF 4, MCF 6) were successfully produced using the hydrothermal method and their electrochemical behavior was studied. The crystallite size was confirmed by XRD, and the grain-like structure was verified by FESEM. The specific capacitance of the material was obtained from the CV curve, yielding a maximum value of 124.28 Fg^{-1} at a scan rate of 5 mV s^{-1} for MCF 2. The results suggest that prepared nanoparticles are anticipated to be very helpful in the fields of supercapacitors, batteries, fuel cells and sensing in future study.

REFERENCES

- [1] D.P. Dubal, P. Gomez-Romero, B.R. Sankapal and R. Holze, *Nano Energy* **11**, 377–399 (2015).
- [2] L.L. Zhang and X.S. Zhao, *Chem. Soc. Rev.* **38**, 2520–2531(2009).
- [3] A. Balducci, R. Dugas, P. Taberna, P. Simon, D. Plee, M. Mastragostino and S. Passerini, *J. Power Sources* **165**, 922–927 (2007).
- [4] T.-F. Yi, L.-Y. Qiu, J. Mei, S.-Y. Qi, P. Cui, S. Luo, Y.-R. Zhu, Y. Xie and Y.-B. He, *Sci. Bull.* **65**, 546–556 (2020).
- [5] N. Padmanathan and S. Selladurai, *Ionics* **20**, 479–487 (2014).
- [6] K.N. Hui, K.S. Hui, Z. Tang, V.V. Jadhav and Q.X. Xia, *J. Power Sources* **330**, 195–203 (2016).
- [7] S. Sahoo, K. Kumar Naik and C. Sekhar Rout, *Nanotechnology* **26**, 455401 (2015).
- [8] L. Li, Y.Q. Zhang, X.Y. Liu, S.J. Shi, X.Y. Zhao, H. Zhang, X. Ge, G.F. Cai, C.D. Gu, X.L. Wang and J.P. Tu, *Electrochim. Acta* **116**, 467–474 (2014).
- [9] G.M. Thorat, H.S. Jadhav and J. Gil Seo, *Ceram. Int.* **43**, 2670–2679 (2017).
- [10] M. Dorri, C. Zamani, and A. Babaei, *J. Ultrafine Grained Nanostruct. Mater.* **51**, 115-122 (2018).
- [11] A.J.C. Wilson, *Acta Crystallogr.* **10**, 88 (1957).
- [12] Y. Zhang, L. Luo, Z. Zhang, Y. Ding, S. Liu, D. Deng, H. Zhao, and Y. Chaen, *J. Mater. Chem. B* **2**, 529-535 (2014).
- [13] D. Cai, B. Liu, D. Wang, Y. Liu, L. Wang, H. Li, Y. Wang, C. Wang, Q. Li and T. Wang, *Electrochim. Acta* **125**, 294–301(2014).
- [14] I. Shakir, M. Shahid, H.W. Yang and D.J. Kang, *Electrochim. Acta* **56**, 376–380 (2010).